Comparative analysis of some models of mixed-substrate microbial growth

Atul Narang*

9th February 2008

Department of Chemical Engineering, University of Florida, Gainesville, FL 32611-6005.

Keywords: Mathematical model, mixed substrate growth, diauxic growth, lac operon, Lotka-Volterra model.

Abstract

Mixed-substrate microbial growth is among the most intensely studied systems in molecular microbiology. Several mathematical models have been developed to account for the genetic regulation of such systems, especially those resulting in diauxic growth. In this work, we compare the dynamics of three such models (Narang, Biotech. Bioeng., 59, 116, 1998; Thattai & Shraiman, Biophys. J, 85, 744, 2003; Brandt et al, Water Research, 38, 1004, 2004). We show that these models are dynamically similar — the initial motion of the inducible enzymes in all the models is described by Lotka-Volterra equations for competing species. In particular, the prediction of diauxic growth corresponds to "extinction" of one of the enzymes during the first few hours of growth. The dynamic similarity occurs because in all the models, the inducible enzymes possess properties characteristic of competing species: Their synthesis is autocatalytic, and they inhibit each other. Despite this dynamic similarity, the models vary with respect to the range of dynamics captured. The Brandt et al model captures only the diauxic growth pattern, whereas the remaining two models capture both diauxic and non-diauxic growth patterns. The models also differ with respect to the mechanisms that generate the mutual inhibition between the enzymes. In the Narang model, the mutual inhibition occurs because the enzymes for each substrate enhance the dilution of the enzymes for the other substrate. In the Thattai & Shraiman model, the mutual inhibition is entirely due to competition for the phosphoryl groups. Elements of all the models appear to be necessary for quantitative agreement with data.

1 Introduction

When microbial cells are grown in a batch culture containing a mixture of two carbon sources, they often exhibit *diauxic* growth, which is characterized by the appearance two exponential growth phases separated by a lag phase called *diauxic lag* [16]. The most well-known example of this phenomenon is the batch growth of *E. coli* on a mixture of glucose and lactose (Figure 1a). Early studies by Monod showed that in this case, the two exponential growth phases reflect the sequential consumption of glucose and lactose [15]. Moreover, only glucose is consumed in the first exponential growth phase because the synthesis of the *peripheral* enzymes for lactose (the enzymes that catalyze the transport and peripheral catabolism of lactose) is somehow abolished in the presence of glucose. During this period of preferential growth on glucose, the peripheral enzymes for lactose are diluted to very small levels: 6–7 generations of growth on glucose reduce the enzyme levels to $\sim 1\%$ of their initial values. Thus, the diauxic lag reflects the time required for the cells to build up the peripheral enzymes for lactose to sufficiently high levels. After the diauxic lag, one observes the second exponential phase corresponding to consumption of lactose.

The key to the resolution of the glucose-lactose diauxie is clearly the molecular mechanism by which the synthesis of lactose-specific enzymes is abolished in the presence of glucose. The first inroads into this

*Email: narang@che.ufl.edu

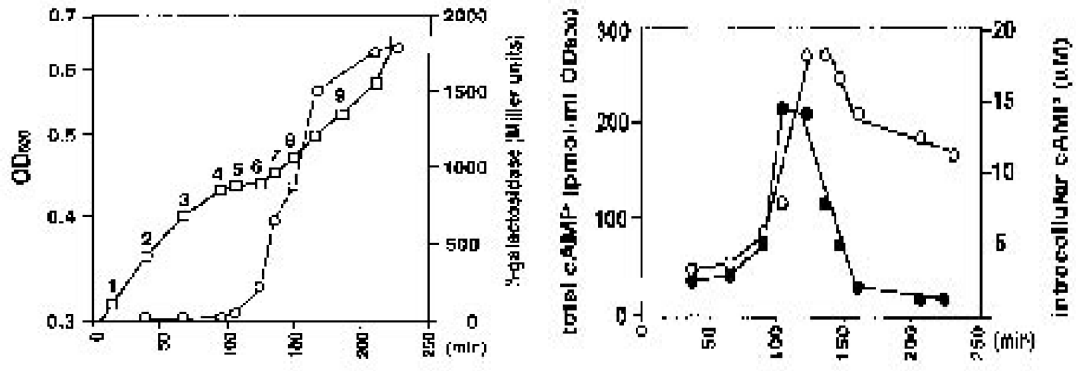

(a) (b)

Figure 1: Diauxic growth of *E. coli* on a mixture of glucose and lactose (from [8]): (a) The optical density (□) shows two exponential growth phases separated by a diauxic lag ($60 \lesssim t \lesssim 160$ min). The levels of β-galactosidase (◯), a peripheral enzyme for lactose, remain low until the beginning of the diauxic lag. (b) Evolution of the intracellular cAMP levels during the experiment shown in (a). The intracellular cAMP levels (•) during the first phase of exponential growth on glucose ($t \lesssim 60$ min) are similar to the intracellular cAMP levels during the second phase of exponential growth on lactose ($t \gtrsim 160$ min).

problem were made by Monod and coworkers who discovered the mechanism for synthesis (induction) of the lactose-specific enzymes in the presence of lactose [10]. It was shown that the genes corresponding to the peripheral enzymes for lactose are contiguous on the DNA, an arrangement referred to as the *lac* operon. In the absence of lactose, transcription of the *lac* operon is prevented by a repressor molecule, called the *lac* repressor, which is bound to a specific site on the *lac* operon. In the presence of lactose, transcription of the *lac* operon is triggered because allolactose, a product of β-galactosidase, sequesters the repressor from the operon, thus liberating it for transcription.[1]

Given this mechanism for induction of the lactose-specific enzymes, it seems plausible to hypothesize that the glucose-lactose diauxie occurs because transcription of the *lac* operon is somehow abolished in the presence of glucose. These mechanisms are not fully understood [28]. Until recently, there were two models for inhibition of *lac* transcription in the presence of glucose

1. *cAMP activation:* This model postulates that a complex consisting of cyclic AMP (cAMP) and catabolite repression protein (CRP) must bind to a specific site on the *lac* operon before it can be transcribed. When glucose is added to a culture growing on lactose, the cAMP levels somehow decrease, which reduces the binding of the cAMP-CRP complex to the *lac* operon, thus inhibiting its transcription rate.

2. *Inducer exclusion:* According to this model, enzyme $\mathrm{IIA^{glc}}$, a peripheral enzyme for glucose, is dephosphorylated in the presence of glucose. The dephosphorylated enzyme $\mathrm{IIA^{glc}}$ inhibits lactose uptake by binding to the lactose permease, the transport enzyme for lactose. This reduces the intracellular concentration of allolactose, and hence, the transcription rate of the *lac* operon.

Experiments by Aiba and coworkers have shown that the cAMP activation model is not tenable [8]. The cAMP levels are the same during growth on glucose and lactose (Figure 1b). Moreover, the *lac* operon is not transcribed even if cAMP is added to a culture growing on glucose and lactose. It is now believed that inducer exclusion alone is responsible for inhibiting *lac* transcription. But in *E. coli* ML30, the activity

[1] A similar mechanism serves to induce the genes for glucose transport [23, Figure 4]. In the absence of glucose, transcription of the *ptsG* gene, which codes for the transport enzyme, $\mathrm{IIBC^{glc}}$, is inhibited because a repressor called Mlc is bound to a regulatory site on the gene. Upon entry of glucose, $\mathrm{IIBC^{glc}}$ is dephosphorylated. Dephosphorylated $\mathrm{IIBC^{glc}}$ sequesters Mlc away from the regulatory site on *ptsG*, thus liberating the gene for transcription.

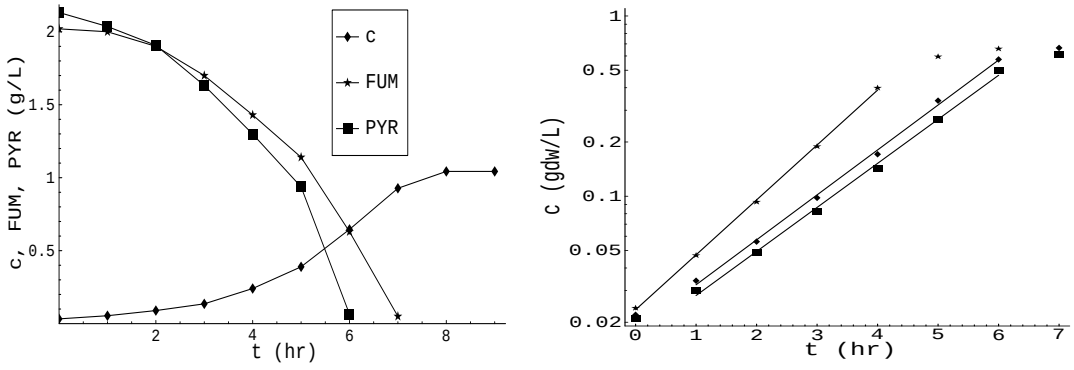

(a) (b)

Figure 2: Nondiauxic growth of *E. coli* (from [21]): (a) Simultaneous substrate utilization during batch growth of *E. coli* K12 on a mixture of fumarate (FUM) and pyruvate (PYR). The cell density is denoted by c (gdw/L) . This growth pattern is observed with several pairs of organic acids [21]. (b) Growth pattern dependent on the history of the inoculum. When the inoculum is grown on glucose ($*$), the specific growth rate on a mixture of glucose and pyruvate is 0.74 1/hr. When the inoculum is grown on pyruvate (■, ♦), the specific growth rate on the same mixture is 0.56 1/hr.

of lactose permease is inhibited no more than ∼40% at saturating concentrations of glucose [3, Table 2]. Likewise, Saier and coworkers, who discovered inducer exclusion in *S. typhimurium*, found that inducer exclusion by glucose inhibits the synthesis of the peripheral enzymes for melibiose, glycerol, maltose, and lactose by 10–50% [26, Figures 1–2]. This partial inhibition by inducer exclusion cannot explain the almost complete inhibition of the genes for the "less preferred" substrates.

Although the diauxie has dominated the literature on mixed-substrate growth, there is ample evidence of non-diauxic growth patterns. This was already evident from Monod's early studies in which he classified his mixed-substrate data into two categories [15, 16]. Growth on a particular mixture was called diauxic if the growth curve showed the diauxic lag, and *normal* if it showed no such lag. Yet, the phenomenon of normal growth was virtually ignored until recently. In the last few years, several studies have shown that both substrates can be consumed simultaneously. Figure 2a shows, for instance, that *E. coli* consumes fumarate and pyruvate simultaneously during batch growth. Egli has summarized all known examples of simultaneous substrate utilization in a comprehensive review article [5]. He notes that, in general, simultaneous substrate utilization is observed when both substrates support low-to-medium specific growth rates, and diauxic growth occurs when one of the substrates supports a specific growth rate that is substantially higher than the specific growth rate on the other substrate. In addition to simultaneous substrate utilization, there is some evidence that the substrate utilization pattern can depend on the history of the inoculum, one example of which is shown in Figure 2b (see [18] for other examples).

The phenomenon of mixed-substrate growth is of fundamental importance in molecular biology as a paradigm of the mechanism by which the expression of DNA is controlled. It also has profound implications for several large-scale biotechnological processes.[2] This has spurred the development of several mechanistic models of mixed-substrate growth. Some of these models are inspired by the detailed, but constantly evolving, knowledge of the molecular mechanism for the glucose-lactose diauxie [27, 30, 31]. The other models appeal to the fact that the phenomenon of diauxic growth is ubiquitous — it has been observed in diverse microbial species on many pairs of *substitutable* substrates (i.e., substrates that satisfy the same nutrient requirements)

[2]The large-scale production of chemicals, such as bioethanol and biopolymers, is economically feasible only if they are derived from cheap lignocellulosic feedstocks [9]. The pretreatment of these feedstocks yields a mixture of hexoses (primarily, glucose) and pentoses (primarily, xylose). The cells that ferment these sugars to useful products typically exhibit diauxic growth with preferential consumption of hexoses.

including pairs of carbon [5, 6, 13], nitrogen [22], and phosphorus [4] sources, and even among pairs of electron acceptors [14]. Thus, it is conceivable there exist some general mechanisms driving the dynamics of mixed-substrate growth. These general models, which abstract features common to many, if not all, mixed-substrate systems, include the cybernetic model [12, 25] and several kinetic models [1, 20, 29].

The original cybernetic model, which was analyzed in [19], cannot capture nondiauxic growth patterns. In this work, we compare the general kinetic models developed by Narang et al [18, 20], Brandt et al [1], and Thattai & Shraiman [29]. Hereafter, we shall refer to these as the N-, B- and T-models, respectively. We show that

1. All the models are similar inasmuch as they exhibit the same general class of dynamics. More precisely, the equations describing the initial evolution of the peripheral enzymes are special cases of the generalized Lotka-Volterra model for competing species. This similarity arises because all the models possess the two defining properties of the Lotka-Volterra model for competing species: *Autocatalysis* (the synthesis of the peripheral enzymes for both substrates is autocatalytic), and *mutual inhibition* (the peripheral enzymes for each substrate inhibit the synthesis of the peripheral enzymes for the other substrate). The existence of this similarity implies that the dynamics of the peripheral enzymes are analogous to the dynamics of the Lotka-Volterra model. In particular, the prediction of diauxic growth by these models corresponds to "extinction" of one of the enzymes.

2. The models differ with respect to the predicted range of dynamics and the mechanism by which they inherit the essential properties of the Lotka-Volterra model.

   (a) The B-model captures only diauxic growth patterns, whereas the N- and T-models capture both diauxic non-diauxic growth patterns

   (b) In the N-model, mutual inhibition arises because each enzyme stimulates the dilution of the other enzyme. On the other hand, in the T-model, the mutual inhibition occurs because the sugar-specific enzymes of the phosphotransferase system compete for phosphoryl groups.

Comparison with experiments suggests that elements of both all the models are required for capturing the data.

2 The models

Before describing the models, it is useful to mention a few points.

1. Although all models contain more or less the same variables, the notation varies considerably from one study to another. To facilitate comparison between the models, we have used the same notation for the variables. We denote the cells, exogenous substrates, inducers, and peripheral enzymes by C, S_i, X_i and E_i, respectively. The concentrations of these entities are denoted by the corresponding lower-case letters, s_i, e_i, x_i and c, respectively.

2. All the models assume the existence of a small *constitutive* or background enzyme synthesis rate that persists even in the absence of the inducer. We neglect this term since it is generally small compared to the *induced* enzyme synthesis rate.

3. The cell density and exogenous substrate concentrations are based on the volume of the culture (gdw/L and g/L, respectively). In contrast, the concentrations of intracellular variables, such as the enzymes and inducers, are based on the dry weight of the cells (g/gdw).

4. The foregoing choice of units implies that if Z is any intracellular entity produced at the rate, r_z^+ g/gdw-hr, and degraded at the rate, r_z^- g/gdw-hr, then the mass balance for z (in g/gdw) is given by the equation
$$\frac{d(zc)}{dt} = \left(r_z^+ - r_z^-\right) c \Rightarrow \frac{dz}{dt} = r_z^+ - r_z^- - \left(\frac{1}{c}\frac{dc}{dt}\right) z.$$
   Here, the last term reflects the dilution of Z due to growth.

We are now ready to describe the key features of the models.

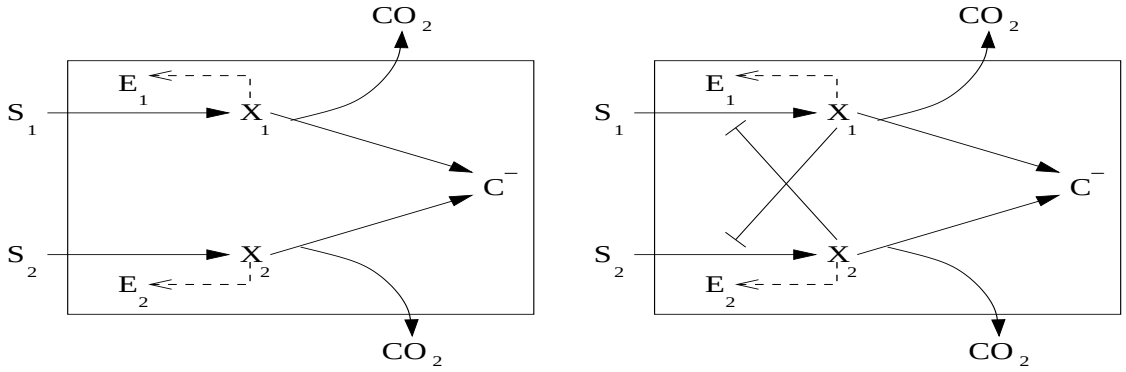

Figure 3: Kinetic schemes: (a) N-model [11]. (b) B-model [18].

2.1 N-model

The kinetic scheme for the N-model is shown in Figure 3a. It is assumed that [18]

1. Transport of S_i is catalyzed by enzyme E_i. The specific uptake rate of S_i, denoted $r_{s,i}$, follows the kinetics, $r_{s,i} \equiv V_{s,i} e_i s_i / (K_{s,i} + s_i)$.
2. Part of the internalized substrate, denoted X_i, is converted to biosynthetic constituents such as amino acids and proteins, denoted C^-. The remainder is oxidized to energy (CO_2).
   (a) The specific rate of conversion of X_i to C^- and CO_2 is $r_{x,i} \equiv k_{x,i} x_i$.
   (b) The fraction of X_i converted to C^- is a constant (parameter), denoted Y_i. Thus, the specific rate of biosynthesis from X_i is $Y_i r_{x,i}$.
3. The internalized substrate induces the synthesis of E_i.
   (a) The specific synthesis rate of E_i is $r_{e,i} \equiv V_{e,i} x_i^{n_i} / (K_{e,i}^{n_i} + x_i^{n_i})$, where $n_i = 1$ or 2.[3]
   (b) The synthesis of the enzymes occurs at the expense of the biosynthetic constituents, C^-.

Thus, one obtains the equations

$$\frac{ds_i}{dt} = -r_{s,i} c,\ r_{s,i} \equiv V_{s,i} e_i \frac{s_i}{K_{s,i} + s_i}, \tag{1}$$

$$\frac{dx_i}{dt} = r_{s,i} - r_{x,i} - \left(\frac{1}{c}\frac{dc}{dt}\right) x_i, r_{x,i} \equiv k_{x,i} x_i, \tag{2}$$

$$\frac{de_i}{dt} = r_{e,i} - \left(\frac{1}{c}\frac{dc}{dt}\right) e_i,\ r_{e,i} \equiv V_{e,i} \frac{x^{n_i}}{K_{e,i}^{n_i} + x^{n_i}}, \tag{3}$$

$$\frac{dc^-}{dt} = (Y_1 r_{x,1} + Y_2 r_{x,2}) - (r_{e,1} + r_{e,2}) - \left(\frac{1}{c}\frac{dc}{dt}\right) c^-. \tag{4}$$

These equations implicitly define the specific growth rate and the evolution of the cell density. To see this, observe that since all the intracellular concentrations are expressed as mass fractions (g/gdw), their sum

[3] Enzyme induction can be hyperbolic ($n_i = 1$) or sigmoidal ($n_i = 2$), depending on the number of inducer molecules that bind to a repressor molecule [2, 32].

equals 1, i.e., $x_1 + x_2 + e_1 + e_2 + c^- = 1$. Hence, addition of equations (2–4) yields

$$0 = \sum_{i=1}^{2} r_{s,i} - (1 - Y_i) r_{x,i} - \frac{1}{c}\frac{dc}{dt}$$

which can be rewritten in the more familiar form

$$\frac{dc}{dt} = r_g c,\ r_g \equiv \sum_{i=1}^{2} r_{s,i} - (1 - Y_i) r_{x,i} \tag{5}$$

where r_g denotes the specific growth rate.

We can simplify the model by observing that $x_i \sim 10^{-3}$ g/gdw [2] and $r_{s,i}, r_{x,i} \sim 1$ g/gdw-hr. Thus, x_i attains quasisteady state on a time scale of 10^{-3} hr. Moreover, the dilution term $r_g x_i \sim 10^{-3}$ g/gdw-hr is negligibly small compared to $r_{s,i}, r_{x,i}$. Hence, within a few seconds, (2) becomes, $0 \approx r_{s,i} - r_{x,i}$, so that $r_g \equiv \sum_i r_{s,i} - (1 - Y_i) r_{x,i} \approx \sum_i Y_i r_{s,i}$. Thus, we arrive at the equations

$$\frac{dc}{dt} = (Y_1 r_{s,1} + Y_2 r_{s,2}) c,\ r_{s,i} \equiv V_{s,i} e_i \frac{s_i}{K_{s,i} + s_i} \tag{6}$$

$$\frac{ds_i}{dt} = -r_{s,i} c \tag{7}$$

$$\frac{de_i}{dt} = r_{e,i} - (Y_1 r_{s,1} + Y_2 r_{s,2}) e_i,\ r_{e,i} \equiv V_{e,i} \frac{x_i^{n_i}}{K_{e,i}^{n_i} + x_i^{n_i}} \tag{8}$$

$$x_i \approx \frac{V_{s,i} e_i s_i / (K_{s,i} + s_i)}{k_{x,i}} \tag{9}$$

$$c^- = 1 - x_1 - x_2 - e_1 - e_2 \tag{10}$$

where (9) is obtained by solving the quasisteady state relation, $r_{x,i} \approx r_{s,i}$, for x_i. Substituting (9) in the expression for $r_{e,i}$ yields

$$r_{e,i} = V_{e,i} \frac{[e_i s_i / (K_{s,i} + s_i)]^{n_i}}{\bar{K}_{e,i}^{n_i} + [e_i s_i / (K_{s,i} + s_i)]^{n_i}},\ \bar{K}_{e,i} \equiv K_{e,i} \frac{k_{x,i}}{V_{s,i}}$$

which shows that enzyme synthesis is autocatalytic: The larger the enzyme level, the higher its synthesis rate. This is a consequence of the cyclic structure associated with the kinetics of induction. Figure 3b shows that the enzyme, E_i, promotes the synthesis of the inducer, X_i, which in turn stimulates the synthesis of even more E_i. This cycle of reactions implies that enzyme synthesis is autocatalytic.

2.2 B-model

The B-model is similar to the N-model, the only difference being that the intracellular substrate, X_i, not only stimulates the induction of E_i, but also inhibits the induction of $E_j, j \neq i$ (shown in Figure 4b as arrows with a bar at one end).[4] Assuming that x_i rapidly attains quasisteady state, Brandt et al arrive at the equations [1]

$$\frac{dc}{dt} = r_g c,\ r_g = r_{g,1} + r_{g,2},\ r_{g,i} \equiv V_{g,i} e_i \frac{s_i}{K_{s,i} + s_i} \tag{11}$$

$$\frac{ds_i}{dt} = -r_{s,i} c,\ r_{s,i} = \frac{r_{g,i}}{Y_i} \tag{12}$$

$$\frac{de_i}{dt} = r_{e,i} - r_g e_i,\ r_{e,i} \equiv r_g \left[\frac{p_i e_i s_i / (K_{s,i} + s_i)}{p_1 e_1 s_1 / (K_{s,1} + s_1) + p_2 e_2 s_2 / (K_{s,2} + s_2)} \right] \tag{13}$$

[4] Brandt et al refer to the intracellular substrate (inducer) and the enzyme induction machinery as *signal molecule* and *synthesizing unit* (SU), respectively (see Figure 1 of [1]).

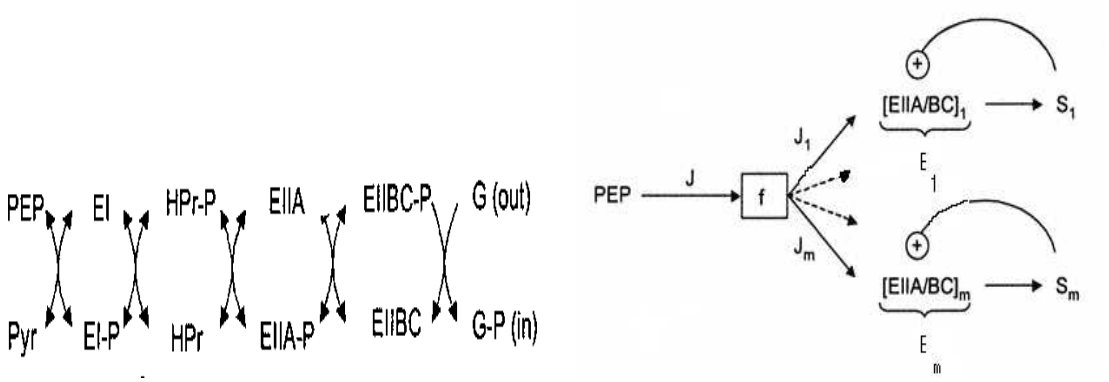

(a) (b)

Figure 4: T-model [29] (a) The phosphotransferase system (PTS) for carbohydrate uptake. (b) The kinetic scheme.

where $r_{g,i}, r_{s,i}, Y_i$ denote the specific growth rate, the specific substrate uptake rate, and the yield of biomass on the i^{th} substrate, r_g denotes the total specific growth rate, and $0 \leq p_i \leq 1$ are parameters called *substrate preference coefficients*.

Evidently, enzyme synthesis is autocatalytic because of the positive feedback from X_i to E_i. The appearance of the specific growth rate, r_g, in the expression for $r_{e,i}$ stems from an additional assumption. It is argued that the specific enzyme synthesis rate should be proportional to the specific growth rate to ensure that the specific enzyme synthesis rate grows in proportion to the specific growth rate.

We note finally that Brandt et al scaled the enzyme level, e_i, with the level, e_i^*, that would be observed during exponential growth on S_i alone. Thus, the variable e_i shown in equation (13) corresponds to the scaled variable, $\kappa_i \equiv e_i/e_i^*$ in [1].

2.3 T-model

The T-model is aimed at describing the evolution of the peripheral enzymes belonging to the *phosphotransferase system* (PTS), which catalyzes the uptake of various sugars in certain bacteria [24]. The uptake of PTS sugars is coupled to their phosphorylation. This is mediated by a cascade of 5 phosphorylation reactions involving the successive transfer of a phosphoryl group from PEP to the sugar (Figure 4a). The first two steps, involving phosphorylation of enzyme I (EI) and HPr, are common to all the PTS sugars. The last three steps are mediated by sugar-specific enzymes, enzyme IIA (EIIA) and the enzyme IIBC complex (EIIBC), which ultimately transfer the phosphoryl group to the sugar during its translocation across the membrane. The sugar-specific enzymes are inducible, and their synthesis is coupled since they lie on the same operon.

Figure 4b shows the kinetic scheme of the T-model. It is assumed that

1. There is a maximum flux, J, of phosphoryl groups through the common enzymes, EI and HPr, and the sugar-specific enzymes of PTS compete for these phosphoryl group. It turns out that at quasisteady state, the specific phosphorylation rate of i^{th} substrate, J_i, (which is equal to the specific substrate uptake rate, $r_{s,i}$) is given by

$$r_{s,i} = J_i = J\frac{\tau_i}{1+\tau_1+\tau_2},\ \tau_i \equiv \frac{e_i^2}{\beta_i}\frac{s_i}{s_i+e_i},$$

where τ_i can be interpreted as the *demand* for phosphoryl groups by the i^{th} sugar — it is an increasing function of the exogenous sugar concentration, s_i, and the sugar-specific enzyme level, e_i. Consistent with this interpretation, $J_i < J$ due to competing demands for phosphoryl groups imposed by the substrates.

2. The specific rate of enzyme synthesis, $r_{e,i}$, is proportional to the concentration of the intracellular substrate (inducer), x_i, which in turn is proportional to the specific substrate uptake rate, $r_{s,i}$. Hence

$$r_{e,i} \propto r_{s,i},$$

which implies that enzyme synthesis is autocatalytic.

3. The substrate concentrations and the specific growth rate are constant — they are treated as parameters.

Thus, the evolution of the sugar-specific enzymes for the i^{th} substrate, when appropriately scaled, is given by the equations [29]

$$\frac{de_i}{dt} = \frac{\tau_i}{1+\tau_1+\tau_2} - e_i,\ \tau_i \equiv \frac{e_i^2}{\beta_i}\frac{s_i}{s_i+e_i}. \tag{14}$$

Note that the specific growth rate does not appear in the equations, since time is scaled by the parameter, $1/r_g$.

3 Results

We wish to compare the dynamics of the three models described above. At first sight, this seems impossible since the T-model describes the dynamics of the enzymes only, whereas the N- and B-models describe the dynamics of the enzymes, substrates, and cells. It turns out, however, that the dynamics of the substrates and cells are irrelevant on the time scale of interest. Indeed, insofar as the dynamics of mixed-substrate growth are concerned, the asymptotic dynamics ($t \to \infty$) of the N- and B-models is of little interest. Much more revealing are their dynamics during the first exponential growth phase, since it is these finite-time dynamics that determine the substrate utilization pattern. Specifically, diauxic growth will occur if the peripheral enzymes for one of the substrates vanishes during the first exponential growth phase. In contrast, simultaneous substrate utilization will be observed if the enzymes for both substrates persist during the first exponential growth phase. We show below that

1. In the N-, and B-models, the motion of the enzymes during the first exponential growth phase can be described by a reduced system of two equations that are formally similar to the equations of the T-model. This makes it possible to compare the N- and B-models with the T-model.

2. The reduced equations of all the models are different realizations of the generalized Lotka-Volterra model for two competing species. Thus, in all the models, the enzymes behave like two competing species. In particular, they coexist or become extinct, and these dynamics have meaningful biological interpretations in the context of mixed-substrate growth.

3. The B-model can never capture non-diauxic growth patterns.

Finally, we compare the mechanisms underlying the dynamics of the N- and T-models.

3.1 All the models are dynamically similar to the Lotka-Volterra model

We begin by showing that in the N- and B-models, the dynamics of the enzymes during the first exponential growth phase can be described by a reduced system of two equations. To see this, observe that during this period, both substrates are in excess, i.e., $s_i \gg K_{s,i}$. Hence, even though the exogenous substrate concentrations are changing, the transport enzymes remain saturated ($s_i/(K_{s,i}+s_i) \approx 1$). Now, the cells sense the environment through the transport enzymes. Since these enzymes see a quasiconstant environment during the first exponential growth phase, they approach quasisteady state levels. It follows that in the N-

and B-models, the motion of the enzymes from any initial conditions to the quasisteady state levels can be obtained from (8) and (13) by replacing $s_i/(K_{s,i}+s_i)$ with 1.[5] Thus, we arrive at the reduced equations

$$\frac{de_i}{dt} = V_{e,i}\frac{e_i^{n_i}}{K_{e,i}+e_i^{n_i}} - (Y_1 V_{s,1} e_1 + Y_2 V_{s,2} e_2)\, e_i \tag{15}$$

$$\frac{de_i}{dt} = r_g\left(\frac{p_i e_i}{p_1 e_1 + p_2 e_2} - e_i\right). \tag{16}$$

Since these equations are formally similar to equation (14), we can compare the dynamics of all three models.

It turns out that the equations of all three models are dynamical analogs of the generalized Lotka-Volterra model for two competing species, which is given by the equations [7, Chapter 12]

$$\frac{dN_i}{dt} = f_i(N_1, N_2)N_i \tag{17}$$

where N_i and $f_i(N_1, N_2)$ denote the population density and specific growth rate of the i^{th} species, respectively, and $f_i(N_1, N_2)$ satisfies the properties

1. $\partial f_1/\partial N_2, \partial f_2/\partial N_1 < 0$, i.e., each species inhibits the growth of the other species.
2. $f_i(N_1, N_2) < 0$ for sufficiently large $N_1, N_2 > 0$, i.e., at sufficiently large population densities, the specific growth rates are negative.

The standard Lotka-Volterra model for competing species is a special case of the generalized model with

$$f_i(N_1, N_2) = r_i(1 - a_{i1}N_1 - a_{i2}N_2)$$

where r_i is the unrestricted specific growth rate of the i^{th} species in the absence of any competition, and a_{i1}, a_{i2} are coefficients that quantify the reduction of the unrestricted specific growth rate due to intra- and inter-specific competition [17]. The analogy between the generalized Lotka-Volterra model and equations (14–16) becomes evident if we rewrite the latter in the form

$$\frac{de_i}{dt} = f_i^N(e_1, e_2)e_i,\ f_i^N(e_1, e_2) \equiv V_{e,i}\frac{e_i^{n_i-1}}{\bar{K}_{e,i}^{n_i} + e_i^{n_i}} - (Y_1 V_{s,1} e_1 + Y_2 V_{s,2} e_2) \tag{18}$$

$$\frac{de_i}{dt} = f_i^B(e_1, e_2)e_i,\ f_i^B(e_1, e_2) \equiv r_g\left(\frac{p_i}{p_1 e_1 + p_2 e_2} - 1\right) \tag{19}$$

$$\frac{de_i}{dt} = f_i^T(e_1, e_2)e_i,\ f_i^T(e_1, e_2) \equiv \frac{e_i s_i/(\beta_i + e_i)}{1 + \tau_1 + \tau_2} - e_i,\ \tau_i \equiv \frac{e_i^2}{\beta_i}\frac{s_i}{s_i + e_i} \tag{20}$$

One can check that the functions, f_i^N, f_i^B, f_i^T satisfy the properties 1 and 2 above. Thus, in all the models, the dynamics of the enzymes during the first exponential growth phase are analogous to the dynamics of the generalized Lotka-Volterra model for two competing species.

The dynamics of the generalized Lotka-Volterra model for competing species are well understood [7, Chapter 12]. Specifically, the model entertains no limit cycles, so that all solutions ultimately converge to some steady state. Despite the absence of limit cycles, the model has a rich spectrum of dynamics. Even in the case of the standard Lotka-Volterra model, one can get 4 different types of dynamics depending on the parameter values [17]. Indeed, if we define the dimensionless variables, $u_i \equiv a_{ii}N_i$ and $\tau \equiv r_1 t$, we obtain the dimensionless equations

$$\frac{du_1}{d\tau} = (1 - u_1 - b_{12}u_2)u_1,\ b_{12} \equiv \frac{a_{12}}{a_{11}}$$

$$\frac{du_2}{d\tau} = \rho(1 - b_{21}u_1 - u_2)u_2,\ \rho \equiv \frac{r_2}{r_1},\ b_{21} \equiv \frac{a_{21}}{a_{22}}.$$

[5] We have reduced the equations by appealing to intuitive arguments. This reduction can be justified rigorously by appealing to the theorem of continuous dependence on initial conditions (see [20] for details).

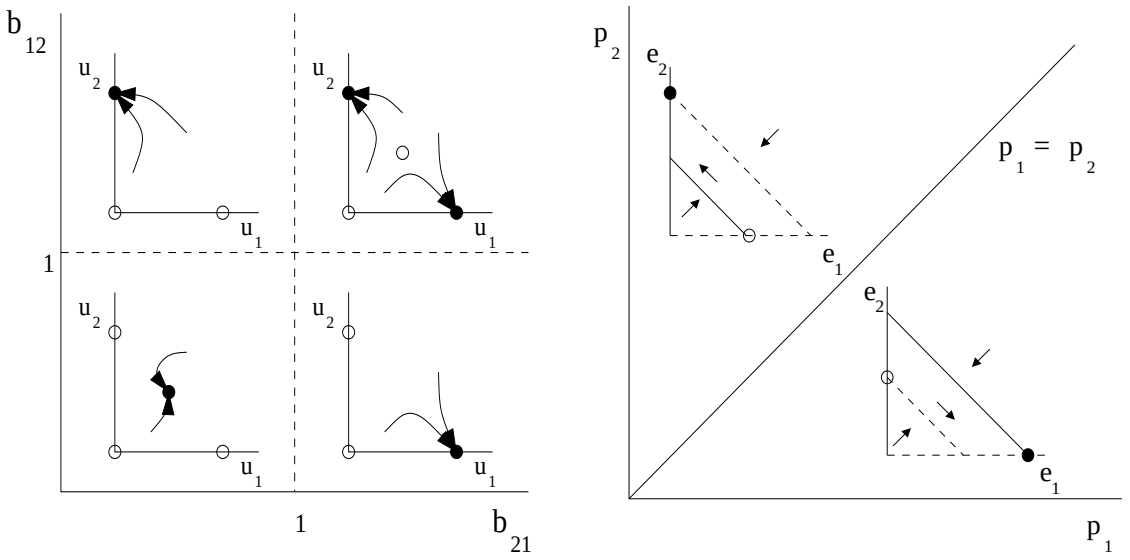

Figure 5: Classification of the global dynamics: (a) The bifurcation diagram of the standard Lotka-Volterra model. The full and open circles show stable and unstable steady states, respectively. (b) The bifurcation diagram of the B-model. When $p_1 > p_2$ (resp., $p_2 > p_1$), E_2 (resp., E_1) is rendered extinct during the first exponential growth phase. The full and dashed lines show the nullclines for e_1 and e_2, respectively. The full and open circles show stable and unstable steady states, respectively. The arrows show the orientation of the vector, $(de_1/dt, de_2/dt)$, in the regions between the nullclines.

The steady states of the model are completely determined by the parameters, b_{ij}, which may be viewed as a measure of the extent to which the j^{th} species inhibits the i^{th} species. Figure 5a shows the bifurcation diagram of the scaled standard Lotka-Volterra model. The bifurcation diagram shows that when neither species inhibits the other species strongly ($b_{12}, b_{21} < 1$), the two species coexist; when the cross-inhibition is asymmetric ($b_{12} > 1, b_{21} < 1$ or $b_{12} < 1, b_{21} > 1$), one of the species is rendered extinct; when both species inhibit each other strongly ($b_{12}, b_{21} > 1$), the outcome of the competition depends on the initial condition.

Given the dynamical analogy between the Lotka-Volterra model and equations (18–20), it is reasonable to expect that the peripheral enzymes would yield similar dynamics during the first phase of exponential growth. Importantly, these dynamics have simple interpretations in terms of the substrate utilization pattern. Indeed, extinction of one of the enzymes during the first phase of exponential growth corresponds to diauxic growth; coexistence of the enzymes during this period is the correlate of simultaneous substrate uptake; and bistability reflects a substrate utilization pattern which varies depending on the manner in which the inoculum has been precultured.

3.2 The B-model cannot capture non-diauxic growth patterns

The N- and T-models can capture diauxic growth, simultaneous substrate utilization, and bistable growth (see [18, 29] for details). However, the B-model always exhibits diauxic growth. Indeed, the dynamics are completely determined by the substrate preference coefficients, p_1 and p_2 (Figure 5b). If $p_1 > p_2$, E_2 becomes extinct during the first exponential growth phase, which corresponds to preferential consumption of S_1. Conversely, if $p_2 > p_1$, E_1 becomes extinct during the first exponential growth phase, which corresponds to preferential consumption of S_2.

To see this, it suffices to consider the nullclines of equation (19), i.e., the curves along which $de_i/dt = 0$.

These curves, which separate the e_1e_2-plane into regions in which de_i/dt is nonzero, are given by the equations

$$e_i = 0 \text{ or } f_i^B(e_1, e_2) \equiv \frac{p_i}{p_1e_1 + p_2e_2} - 1 = 0,\ i = 1, 2.$$

Evidently, $de_1/dt = 0$ along the e_2-axis and the straight line, $p_1e_1 + p_2e_2 = p_1$; we shall refer to the latter curve as μ. Likewise, $de_2/dt = 0$ along the e_1-axis and the straight line, $p_1e_1+p_2e_2 = p_2$; we shall refer to the latter curve as ν. The steady states of (19) lie at the intersection points of the nullclines for e_1 and e_2. Since μ and ν are parallel, there are no "coexistence" steady states. There are "extinction" steady states at$(1, 0)$ and $(0, 1)$.[6] One can check that the stability of $(1, 0)$ and $(0, 1)$ is determined by the disposition of μ and ν. If $p_1 > p_2$, then μ lies above ν, and $(1, 0)$ is stable, while $(0, 1)$ is unstable. Conversely, if $p_1 < p_2$, then ν lies above μ, and $(0, 1)$ is stable, while $(1, 0)$ is unstable. Thus, we conclude that the B-model entertains only the diauxic growth pattern.

3.3 The N- and T-models have different mechanisms of mutual inhibition

We have shown above that all the models are different realizations of the generalized Lotka-Volterra model for two competing species. Furthermore, the B-model cannot capture the non-diauxic growth patterns. In what follows, we consider the similarities and differences between the N- and T-models.

We can develop a better appreciation of the similarities and differences by examining the manner in which these models acquire the properties of the generalized Lotka-Volterra model. The latter is characterized by two essential properties.

1. The growth of each species is autocatalytic, i.e., $dN_i/dt = 0$ whenever $N_i = 0$.
2. The interaction between the two species is *mutually inhibitory*, i.e, $\partial f_1/\partial N_2, \partial f_2/\partial N_1 < 0$.

It is clear that all the models satisfy the first property precisely because enzyme synthesis is autocatalytic ($r_{e,i} = 0$ whenever $e_i = 0$). The mechanism that ensures that existence of this property is also identical in all the models. It stems from the fact that the enzyme promotes the formation of the internalized substrate (inducer) which in turn stimulates the synthesis of even more enzyme.

The difference between the models lies the mechanism(s) leading to the second property, namely, mutual inhibition. In the N-model, each enzyme inhibits the other enzyme by stimulating growth, and thus increases the rate of *dilution* of the other enzyme (e.g., $\partial f_1^N/\partial e_2 < 0$ precisely because e_2 appears in the dilution term for e_1). On the other hand, in the T-model, there is no mutual inhibition due to dilution — in fact, the specific growth rate is assumed to be a constant parameter. Instead, each enzyme inhibits the rate of *synthesis* of the other enzyme (e.g., $\partial f_1^T/\partial e_2 < 0$ precisely because e_2 appears in the synthesis term for e_1), and this inhibition occurs due to competition for the phosphoryl groups.

The N-model has two advantages over the T-model.

1. It is more general than the T-model since it applies to any pair of inducible substrates, as opposed to PTS sugars only. Indeed, the N-model appeals to the two processes — enzyme induction and growth — that occur in every system involving inducible substrates.

2. It explains an important empirical correlation observed in mixed-substrate growth. Based on a comprehensive review of the experimental literature, Harder & Dijkhuizen [6] and Egli [5] have observed that in general, both substrates are consumed simultaneously when they support low-to-medium single-substrate growth rates. On the other hand, diauxic growth is typically observed when one of the substrates supports a much higher specific growth rate. In this case, the substrate supporting the higher specific growth rate is usually the "preferred substrate."
   This can be understood in terms of the N-model, wherein each enzyme inhibits the other enzyme by enhancing the latter's dilution rate. Thus, enzymes for two substrates that support low-to-medium growth rates will coexist since they will not inhibit each other significantly. However, if the two substrates, say S_1 and S_2, support high and low specific growth rates, respectively, then E_1 will strongly inhibit the synthesis of E_2, but E_2 will have little inhibitory effect on synthesis of E_1. Consequently, E_1 will drive E_2 to "extinction," resulting in preferential utilization of S_1.

[6] There is no steady state at $(0, 0)$ since the model is undefined (discontinuous) at this point.

The disadvantage of the N-model is that, unlike the T-model, it does not account for inhibition of enzyme synthesis. It is conceivable that this occurs by competition for phosphoryl groups. Another mechanism, well-documented in the experimental literature, is inducer exclusion [28]. The latter is not accounted for by the N- and T-models. Indeed, neither one of these models accounts for direct interaction between the enzymes for the two substrates. The effect of the enzymes belonging to the other substrate are exerted indirectly by influencing the specific growth rate or demand for the phosphoryl groups. Thus, the N-model can be viewed as a general model which is true of every pair of substrates with inducible peripheral enzymes. However, for quantitative agreement, it must be modified along the lines of the T-model by accounting for specific mechanisms, such as inducer exclusion and competition for phosphoryl groups, that inhibit enzyme synthesis.

It is striking that all the models can predict diauxic growth despite the absence of direct inhibitory interactions such as inducer exclusion. These dynamics occur precisely because enzyme synthesis is autocatalytic — it is this property that makes it feasible for enzymes to become "extinct" during the first exponential growth phase. Thus, the models imply that diauxic growth would not be observed if autocatalysis were destroyed. This is consistent with the experimental data. Constitutive mutants, in which synthesis of lactose-specific enzymes persists even in absence of the inducer concentration ($r_{e,i}|_{e_i=0} > 0$), do not display the diauxie [8, Figure 6]. Similarly, the glucose-lactose diauxie is not observed if the medium contains IPTG, an inducer of the *lac* operon that can enter the cell even in the absence of the lactose permease [8, Figure 7].

4 Conclusions

We compared the similarities and differences between three kinetic models of mixed-substrate growth. We showed that

1. In all three models, the dynamics of the peripheral enzymes are formally similar to the generalized Lotka-Volterra model for competing species. This similarity occurs because the peripheral enzymes mirror the two essential properties of the Lotka-Volterra model: (a) Synthesis of the peripheral enzymes for both substrates are autocatalytic (b) The peripheral enzymes for the two substrates inhibit each other.

2. The model by Brandt et al [1] cannot capture non-diauxic growth patterns. For all parameter values, the peripheral enzymes for one of the substrates becomes extinct during the first exponential growth phase, thus resulting in diauxic growth.

3. The models in [18] and [29] capture both diauxic and non-diauxic growth patterns. Both models are identical with respect to the mechanism that ensures that peripheral enzyme synthesis is autocatalytic — the peripheral enzymes promote the synthesis of the inducer, which in turn stimulates the synthesis of even more enzyme. However, they differ with respect to the mechanism that produces mutual inhibition. In the Narang model, the mutual inhibition occurs because each enzyme stimulates the dilution rate of the other enzyme. In the Thattai & Shraiman model, which applies to PTS sugars only, the mutual inhibition stems from competition for phosphoryl groups.

References

[1] B. W. Brandt, F. D. L. Kelpin, I. M. M. van Leuwen, and S. A. L. M. Kooijman. Modelling microbial adaptation to changing availability of substrates. *Water Research*, 38:1004–1013, 2004.

[2] J. D. Chung and G. Stephanopoulos. On physiological multiplicity and population heterogeneity of biological systems. *Chem. Eng. Sc.*, 51:1509–1521, 1996.

[3] M. Cohn and K. Horibata. Inhibition by glucose of the induced synthesis of the β-galactoside-enzyme system of *Escherichia coli*. Analysis of maintenance. *J. Bacteriol.*, 78:601–612, 1959.

[4] C. G. Daughton, A. M. Cook, and M. Alexander. Phosphate and soil binding: factors limiting bacterial degradation of ionic phosphorus-containing pesticide metabolites. *Appl Environ Microbiol*, 37(3):605–609, Mar 1979.

[5] T. Egli. The ecological and physiological significance of the growth of heterotrophic microorganisms with mixtures of substrates. *Adv. Microbiol. Ecol.*, 14:305–386, 1995.

[6] W. Harder and L. Dijkhuizen. Strategies of mixed substrate utilization in microorganisms. *Philos. Trans. R. Soc. London B*, 297:459–480, 1982.

[7] M. W. Hirsch and S. Smale. *Differential Equations, Dynamical Systems, and Linear Algebra*. Academic Press, New York, 1974.

[8] T. Inada, K. Kimata, and H. Aiba. Mechanism responsible for the glucose-lactose diauxie in *Escherichia coli*: Challenge to the cAMP model. *Genes Cells*, 1:293–301, 1996.

[9] L. O. Ingram, H. C. Aldrich, A. C. C. Borges, T. B. Causey, A. Martinez, F. Morales, A. Saleh, S. A. Underwood, L. P. Yomano, S. W. York, J. Zaldivar, and S. Zhou. Enteric bacterial catalysts for fuel ethanol production. *Biotechnol. Prog.*, 15:855–866, 1999.

[10] F. Jacob and J. Monod. Genetic regulatory mechanisms in the synthesis of proteins. *J. Mol. Biol.*, 3: 318–356, 1961.

[11] D. S. Kompala, D. Ramkrishna, N. B. Jansen, and G. T. Tsao. Investigation of bacterial growth on mixed substrates: Experimental evaluation of cybernetic models. *Biotechnol. Bioeng.*, 28:1044–1055, 1986.

[12] D. S. Kompala, D. Ramkrishna, and G. T. Tsao. Cybernetic modeling of microbial growth on multiple substrates. *Biotechnol. Bioeng.*, 26:1272–1281, 1984.

[13] K. Kovarova-Kovar and T. Egli. Growth kinetics of suspended microbial cells: From single-substrate-controlled growth to mixed-substrate kinetics. *Microbiol. Mol. Biol. Rev.*, 62:646–666, 1998.

[14] P. H. Liu, S. A. Svoronos, and B. Koopman. Experimental and modeling study of diauxic lag of Pseudomonas denitrificans switching from oxic to anoxic conditions. *Biotechnol Bioeng*, 60(6):649–655, Dec 1998.

[15] J. Monod. Recherches sur la croissance des cultures bactériennes [Studies on the growth of bacterial cultures]. *Actualités Scientifique et Industrielles*, 911:1–215, 1942.

[16] J. Monod. The phenomenon of enzymatic adaptation and its bearings on problems of genetics and cellular differentiation. *Growth*, 11:223–289, 1947.

[17] J. D. Murray. *Mathematical Biology*. Biomathematics Texts. Springer-Verlag, New York, 1989.

[18] A. Narang. The dynamical analogy between microbial growth on mixtures of substrates and population growth of competing species. *Biotechnol. Bioeng.*, 59:116–121, 1998.

[19] A. Narang, A. Konopka, and D. Ramkrishna. Dynamic analysis of the cybernetic model for diauxic growth. *Chem. Eng. Sc.*, 52:2567–2578, 1997.

[20] A. Narang, A. Konopka, and D. Ramkrishna. The dynamics of microbial growth on mixtures of substrates in batch reactors. *J. Theor. Biol.*, 184:301–317, 1997.

[21] A. Narang, A. Konopka, and D. Ramkrishna. New patterns of mixed substrate growth in batch cultures of *Escherichia coli* K12. *Biotechnol. Bioeng.*, 55:747–757, 1997.

[22] F. C. Neidhardt and B. Magasanik. Reversal of the glucose inhibition of histidase biosynthesis in Aerobacter aerogenes. *J Bacteriol*, 73(2):253–259, Feb 1957.

[23] J. Plumbridge. Regulation of gene expression in the PTS in *Escherichia coli*: The role and interactions of Mlc. *Curr. Opin. Microbiol.*, 5:187–193, 2003.

[24] P. W. Postma, J. W. Lengeler, and G. R. Jacobson. Phosphoenolpyruvate:carbohydrate phosphotransferase systems of bacteria. *Microbiol Rev*, 57(3):543–594, Sep 1993.

[25] R. Ramakrishna, D. Ramkrishna, and A. E. Konopka. Cybernetic modeling of growth in mixed, substitutable substrate environments: Preferential and simultaneous utilization. *Biotechnol. Bioeng.*, 52: 141–151, 1996.

[26] M. H. Saier and S. Roseman. Inducer exclusion and repression of enzyme synthesis in mutants of Salmonella typhimurium defective in enzyme I of the phosphoenolpyruvate: sugar phosphotransferase system. *J Biol Chem*, 247(3):972–975, Feb 1972.

[27] Moisés Santillán and Michael C Mackey. Influence of catabolite repression and inducer exclusion on the bistable behavior of the lac operon. *Biophys J*, 86(3):1282–1292, Mar 2004.

[28] J. Stülke and W. Hillen. Carbon catabolite repression in bacteria. *Curr. Opin. Microbiol.*, 2:195–201, 1999.

[29] Mukund Thattai and Boris I Shraiman. Metabolic switching in the sugar phosphotransferase system of *Escherichia coli*. *Biophys J*, 85(2):744–754, Aug 2003.

[30] G. van Dedem and M. Moo-Young. Cell growth and extracellular enzyme synthesis in fermentations. *Biotechnol. Bioeng.*, 15:419–439, 1973.

[31] P. Wong, S. Gladney, and J. D. Keasling. Mathematical model of the *lac* operon: Inducer exclusion, catabolite repression, and diauxic growth on glucose and lactose. *Biotechnol. Prog.*, 1997.

[32] G. Yagil and E. Yagil. On the relation between effector concentration and the rate of induced enzyme synthesis. *Biochem. J.*, 11:11–17, 1971.